Nobiletin selectively inhibits oral cancer cell growth by promoting apoptosis and DNA damage in vitro

Junjun Yang,[a] Yang Yang,[b] Lu Wang,[c] Qiuchen Jin,[a] and Minghui Pan[a]

Objectives. The aim of this study was to investigate whether nobiletin (NOB) can inhibit the proliferation of oral squamous cell carcinoma (OSCC) cells by promoting apoptosis, oxidative stress (reactive oxygen species [ROS]), and DNA damage.

Study Design. OSCCs were treated with different concentrations of NOB (25, 50, and 100 μM) for different amounts of time (0, 24, 48, and 72 hours). The viability of NOB was assessed by using MTT-based cell viability assays. Flow cytometry was used to assess cell apoptosis, and the expressions of capase-3 and poly (adenosine diphosphate-ribose) polymerase (PARP) were assessed by quantitative real-time polymerase chain reaction (qRT-PCR) and Western blot analyses. The intensity of ROS fluorescence was measured by using a spectrophotometer. The expression of γH2AX and 8-Oxo-20-deoxyguanosine (8-oxodG) were assessed to determine the degree of DNA damage.

Results. We observed that NOB decreased OSCC cell viability in a dose- and time-dependent manner but had little effect on primary normal human oral epithelial cells (H0 ECs). Moreover, with the increase in NOB concentration and treatment time, capase-3, PARP messenger RNA (mRNA), and protein levels gradually increased, as did annexin V- and 7 adducin (ADD)−mediated apoptosis. In addition, NOB also increased the levels of ROS and DNA damage in a concentration- and time-dependent manner.

Conclusions. NOB can inhibit OSCC cell by promoting apoptosis, ROS production, and DNA damage. (Oral Surg Oral Med Oral Pathol Oral Radiol 2020;130:419−427)

Oral cancer is a common malignancy worldwide, and in addition to surgery, chemotherapy is used as an adjuvant treatment for oral cancer.[1] However, because of nonselectivity between normal and tumor cells, chemotherapy occasionally generates some side effects in patients with oral cancer.[2,3] Therefore, the identification of new drugs and treatment strategies to compensate for, or reverse, the shortcomings of existing treatment methods is a hot spot in the field of oral medicine research.

For a long time, traditional Chinese medicine has been used to treat cancer and may offer some advantages in cancer therapy by either inhibiting cancer cell proliferation or reducing the side effects of chemoradiotherapy.[4] Several natural products have been shown to exhibit preferential killing against cancer cells while allowing normal cells to remain healthy.[5] Therefore, discovery of drugs from traditional Chinese medicine is an attractive approach for the development of anticancer therapeutics. NOB is a bioactive polymethoxylated flavone (5,6,7,8,3',4'−hexamethoxyflavone) that is abundant in the peels of citrus fruits, such as *Citrus depressa* (shiikuwasa), *C. sinensis* (oranges), and *C. limon* (lemons)[6,7] and has been shown to have multiple biologic activities.[8,9] For instance, NOB can significantly inhibit cell apoptosis and the production of reactive oxygen species (ROS) and prevent myocardial ischemia/reperfusion (I/R) injury and ischemic heart disease.[10] NOB can also activate autophagy and mitochondrial function through the sirtuin-1 (SIRT-1)/Forkhead box O3 (FOXO3 α) and peroxisome proliferator−activated receptor γ coactiva-tor-1 alpha (PGC-1 α) pathways in hepatic ischemia and reperfusion injury.[9] In addition, a considerable number of reports have shown that NOB exhibits anticarcinogenic activity against various cancer cells,[11-13] including colon,[14,15] prostate,[16] and lung[17,18] cancers. For example, NOB can promote cell cycle arrest, induce apoptosis, and profoundly modulate signaling proteins associated with cell proliferation and cell death to significantly inhibit the growth of human colon cancer cells.[14] With respect to hepatocellular carcinoma, NOB can induce cell cycle arrest and apoptosis and promote

Statement of Clinical Relevance

Oral cancer is a common malignancy in the world. It is very important to find a drug that can kill oral cancer cells without damaging normal cells. Nobiletin (NOB) can inhibit different cancer cells, but its effect on oral cancer cells remains unclear. The main purpose of our study is to investigate whether NOB can inhibit the proliferation of oral cancer cells and to provide new ideas for the treatment of oral cancer.

[a]Department of Stomatology, The Central Hospital of Wuhan, Wuhan, China.
[b]Department of Pathology, The Central Hospital of Wuhan, Wuhan, China.
[c]Department of Stomatology, Hubei Provincial Hospital of Traditional Chinese Medicine, Hongshan District, Wuhan, China.
Received for publication Dec 30, 2019; returned for revision May 12, 2020; accepted for publication Jun 26, 2020.

2212-4403/$-see front matter
https://doi.org/10.1016/j.oooo.2020.06.020

changes in the expression of proteins, including B-cell lymphoma-2 (Bcl−2), Bax, cleaved caspase−3, and cyclooxygenase 2 (COX−2).[19] Interestingly, NOB has weak antiproliferative activity against normal cell lines but can strongly inhibit the proliferation of several cancer cell lines.[20] A combination of NOB and chemotherapy has been shown to significantly increase the efficacy of the latter, partly counteracting resistance to chemotherapy.[21]

Although NOB has been reported to exhibit antitumor activity against different cancer cells,[17,22] its effect on oral cancer cells remains unclear. Therefore, the primary goal of this study was to investigate whether NOB can inhibit the proliferation of oral cancer cells by increasing apoptosis, ROS, and DNA damage in oral cancer cells in vivo.

MATERIALS AND METHODS

Reagents

NOB (≥ 98%) (Hengfei Biological Technology Co., Ltd., Shanghai, China) was dissolved in 0.5% dimethyl sulfoxide (DMSO) and stored at 4˚C until use. The Ca9-22, HSC-3, TSC-15, and HOECs cell lines were purchased from Wuhan Vicsay Technology Co., Ltd. (Wuhan, China); 10% fetal bovine serum (Gibco, Gaithersburg, MD), phosphate-buffered saline(Procell, Wuhan, China), Dulbecco's Modified Eagle Medium (DMEM medium; Procell, Wuhan, China), and trypsin (AtaGenix, Wuhan, China) were purchased from Wuhan Yipu Biological Technology Co., Ltd.; Annexin V-FITC (Biovision, Milpitas, CA), lysis buffer (Biovision, Milpitas, CA), Culture plates (Trevigen, Gaithersburg, MD), 96-well well plates (Trevigen, Gaithersburg, MD), 6-well plates (Trevigen, Gaithersburg, MD) and complementary DNA (cDNA) synthesis kit (Solis BioDyne, San Diego, CA) were purchased from Amyjet Technology Co., Ltd.; 7-AAD (BioGems, Westlake Village, CA) was purchased from Beijing Luyuan Bird Biotechnology Co., Ltd.; ROS assay kits (Jingke, Shanghai, China) were purchased from Shanghai Jingke Chemical Technology Co., Ltd.; enzyme-linked immunosorbent assay (ELISA) kits (Aviva Systems Biology, Beijing,China) were purchased from Beijing Ovia Biotechnology Co., Ltd.; an ELISA kit (ATCC, Manassas, VA) was purchased from Shanghai Xinyu Biotechnology Co., Ltd.; a chemiluminescence kit (Biorbyt, Cambridge, UK) was purchased from Wuhan Boote Biotechnology Co., Ltd.; serum-free medium (Sigma, St. Louis, MO) was purchased from Shanghai Beinuo Biotechnology Co., Ltd.; TRIzol reagent (Purity Bio, Wuhan, China), SYBR green master mix kit (Purity Bio, Wuhan, China), and apoptosis kit (Purity Bio, Wuhan, China) were purchased from Wuhan Purity Biotechnology Co., Ltd.; the MTT solution (AMEKO, Shanghai, China) was purchased from Shanghai Lianshuo Biological Technology Co., Ltd.; ROS fluorescent probe DCFH-DA (Sigma, St. Louis, MO) was purchased from Shanghai Ruisai Biotechnology Co., Ltd.; and anti-PARP, anti-capase-3, anti-γH2 AX (AtaGenix, Wuhan, China) was purchased from Wuhan Yipu Biological Technology Co., Ltd.

Cell culture

Human OSCC cell lines (Ca9-22, HSC-3, and TSC-15) and primary normal human oral epithelial cells (H0 ECs) stored in liquid nitrogen (Frontier Lab, Japan) were resuscitated and then inoculated into the DMEM medium. The cells were cultured in an incubator at 37˚C under an atmosphere with 5% carbon dioxide. After 24 hours, the cells adhered to the wall, indicating that the recovery was successful. After 2 days, the cells were trypsinized to generate cell suspensions for experiments. The cells were then cultured with DMEM containing 10% fetal bovine serum. After the cells reached the logarithmic growth phase, trypsin was used for digestion and expansion. The expanded cells were then seeded in culture plates and grouped.

Cell viability analysis

Ca9-22, HSC-3, and TSC-15 cells and hOECs in the logarithmic growth phase were harvested, resuspended, and seeded in 96-well plates (200 μL per well). When the bottom of the 96-well flat bottom plate became covered with cells, 100 μL of DMEM culture solution containing NOB at concentrations of 25, 50, and 100 μM was added, and the cells were cultured for 24, 48, and 72 hours. Then, 20 μL of MTT solution (5 mg/mL) was added to each well, and the cells were incubated for 4 hours. Subsequently, the absorbance value of each well at 570 nm was determined by using a microplate reader (Molecular Devices, San Jose, CA), and the inhibition rate (IR) value was calculated according to the following cellular IR formula: IR = (1 − value of drug group A ÷ value of control group A) × 100%.

Detection of apoptosis with annexin V/7-AAD flow cytometry

7-AAD (7-amino-actinomycin D) can be used to detect cell viability because of its ability to bind to the DNA of damaged plasma membranes or nonmetabolizing cells to form highly fluorescent adducts. The cells were seeded into 6-well plates at a density of 5×10^5 cells/mL. When the degree of cell fusion was approximately 70%, the cells were treated with NOB at concentrations of 25, 50, or 100 μM for 24, 48, and 72 hours. Then, the cells were washed twice with phophate-buffered saline, centrifuged (Sigma, Germany) and collected.

Subsequently, the cells were resuspended in 500 μL of binding buffer, after which 10 μL of annexin V-FITC and 5 μL 7-AAD were added and mixed by shaking. The samples were then incubated for 5 minutes in the dark, after which a flow cytometer (BD FACSCanto II; Biosciences Corp., Piscataway, NJ) was used for detection. The flow cytometry data was analyzed by using DIVA (Data-Interpolating Variational Analysis), and in the flow figure, the upper-right quadrant shows cells in late apoptosis, while the lower-right quadrant shows cells in early apoptosis.

Quantitative real-time PCR

We used qRT-PCR to assess messenger RNA (mRNA) levels as previously described. Total RNA was extracted from oral cancer cells by using TRIzol reagent after the indicated treatments. Then, mRNA was reverse transcribed into cDNA by using a commercial cDNA synthesis kit. qRT-PCR was then conducted by using a SYBR green master mix kit on a 7500 system ABI Prism system (ABI Life ProFlex3 × 32, Appbice Applied Biosystems Trading Co., Ltd., Shanghai, China). The PCR thermocycling conditions were as follows: 50˚C for 2 minutes and 95˚C for 10 minutes, followed by 40 cycles of 95˚C for 30 seconds and 60˚C for 30 seconds. mRNA expressions of PPAR, caspase-3, caspase-8, caspase-9, and rH2 AX were normalized to that of GAPDH (glyceraldehyde 3-phosphate dehydrogenase). The primers used in this study were as follows: caspase-3
forward: 5‘-TGGAATGTCAGCTCGCAATG-3′, reverse: 5‘-CAGGTCCGTTCGTTCCAAAA-3′; human GAPDH forward: 5−GAGTCAACGGATTTGGTCGT; reverse: 5−TTGATTTTGGAGGGATCTCG. Experiments were repeated at least three times.

Western blotting

For Western blotting assays, the cells were collected, lysed with lysis buffer, and incubated at 4˚C for 20 minutes. Then, the protein concentration was determined by using a Bio-Rad analysis system (Bio-Rad, Hercules, CA). For each sample, the same amount of total protein (50 μg) was separated by using gel electrophoresis, after which the proteins were transferred to a membrane that was blocked and then incubated with the appropriate the antibodies: PARP (1:2000 dilution), Capase-3 (1:1000 dilution), γH2 AX (1:1000 dilution), and GAPDH (1:10000 dilution). Subsequently, the signal was detected by using an enhanced chemiluminescence kit (Boster, Wuhan, China).

Detection of intracellular ROS

The DCFH-DA (2,7-dichlorodihydrofluorescein diacetate) assay was used to detect ROS generation. The cells from the treatments described above were seeded into a 96-well plate, and the DCFH-DA solution was diluted 1:1000 to 10 mmol/L with serum-free medium. Then, the diluted DCFH-DA solution was added to each well at a final concentration of 10 μM; after incubating for 30 minutes, the cells were treated with DMSO or 25, 50, or 100 μM NOB for 24, 48, and 72 hours. After collecting the cells, the OD (optical density) of the samples was measured with a fluorescence spectrophotometer (HZbscience, Shanghai, China) by using excitation and emission wavelengths of 488 and 525 nm, respectively, to detect the fluorescence intensity before and after stimulation.

8-Oxo-20-deoxyguanosine measurement

We assessed DNA damage by determining the 8-Oxo-20-deoxyguanosine (8-oxodG) levels in cell cultures. The concentration of 8-oxodG was measured in oral cancer cells 24 hours after NOB was detected by using an ELISA kit according to the manufacturer’s instructions.

Statistical analysis

Statistical analyses were performed by using GraphPad Prism Software version 5.0. All of the experiments were repeated at least 3 times, and the quantitative data were expressed as the means ± standard deviation (SD). One-way analysis of variance (ANOVA) was used for comparisons among groups. For each assay, $n > 3$ and $P < .05$ were considered to represent significant changes.

RESULTS

Viability of NOB-treated OSCC cells and primary hOECs

The MTT assay was used to assess the viabilities of Ca9-22, HSC-3, and TSC-15 cells and hOECs treated with DMSO or 25, 50, and 100 μM NOB for 72 hours. As the concentration of NOB increased, the viabilities of Ca9-22, HSC-3, TSC-15, and OSCC cells decreased, and the inhibitory effect became increasingly significant ($n > 3$; $P < .05$) (Figure 1A). However, NOB had no effect on hOECs, showing that the inhibition of OSCC cells by NOB occurs in a dose-dependent manner. Ca9-22, HSC-3, and TSC-15 cells as well as primary hOECs were treated with 50 μM NOB for 24, 48, and 72 hours. As the incubation time with NOB increased, the viabilities of Ca9-22, HSC-3, and TSC-15 cells decreased, and the inhibitory effect became more significant with the increase in treatment time ($n > 3$; $P < .05$) (Figure 1B). However, NOB had no effect on hOECs, indicating that NOB inhibits OSCC cells in a time-dependent manner.

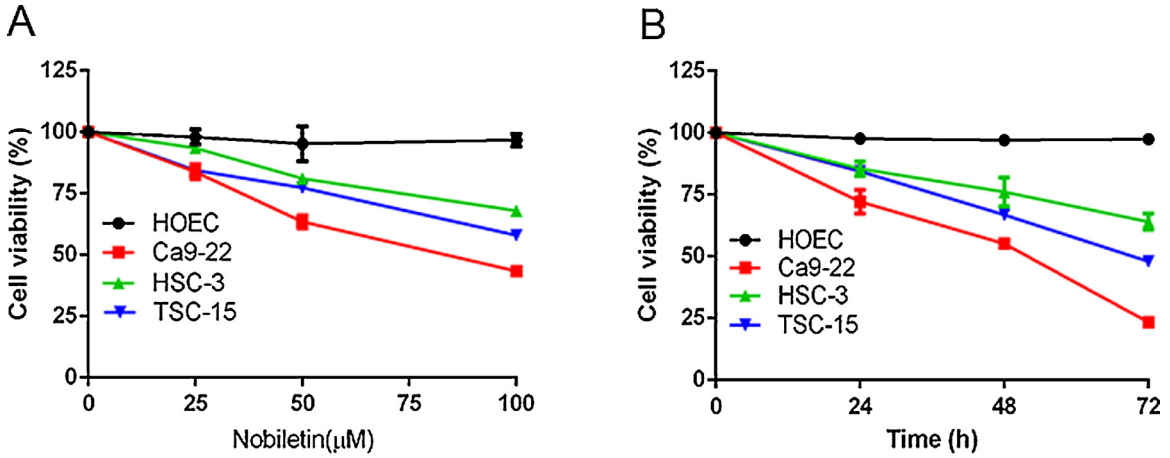

Fig. 1. Viabilities of nobiletin (NOB)−treated oral cancer cells. **A,** Cells were treated with dimethyl sulfoxide (DMSO) or 25, 50, or 100 μM of NOB for 72 hours ($n > 3$; $P < .05$). **B,** Cells were treated with 50 μM of NOB for 24, 48, or 72 hours. ($n > 3$; $P < .05$).

Effect of NOB on the apoptosis of OSCC cells

First, the effects of different concentrations of NOB (25, 50, and 100 μM) and of DMSO on the apoptosis of Ca9-22 cells for 72 hours was detected by flow cytometry (Figures 2A and 2B). The results showed that the DMSO-treated group had the lowest apoptotic rate, and as the NOB concentration increased, the apoptotic rate gradually increased ($n > 3$; $P < .05$), indicating that the ability of NOB to inhibit Ca9-22 oral cancer cells is concentration dependent. Then, the mRNA and protein expressions of PARP and caspase-3 in each group were detected by using PCR and Western blotting (Figures 2C to 2G). The results showed that as the NOB concentration increased, the expression of PARP and caspase-3 increased ($n > 3$; $P < .05$), indicating that NOB can promote cell apoptosis in a concentration-dependent manner.

Subsequently, the effects of a 50 μM NOB treatment for different times (0, 24, 48, and 72 hours) on the apoptosis of Ca9-22 cells were assessed by flow cytometry (Figures 3A and 3B). The results showed that with the increase in time, the apoptotic rate gradually increased ($n > 3$; $P < .05$), indicating that the ability of NOB to inhibit Ca9-22 cells depends on the treatment time. In addition, the expression of PARP and caspase-3 mRNA and protein in each group all increased with time ($n > 3$; $P < .05$) (Figures 3C to 3G), indicating that NOB can promote cell apoptosis in a time-dependent manner.

ROS generation in NOB-treated Ca9-22 cells

To examine the effects of different concentrations of NOB on oxidative stress in cells after 72 hours, we examined the production of ROS in each group of cells. We used a multifunctional fluorescence microplate reader to detect ROS levels in the 4 groups of cells. The data analysis results showed that compared with the DMSO-treated group, the intracellular ROS level increased with the increase in the NOB concentration, and the difference was significant ($n > 3$; $P < .01$). Figure 4A shows the ROS-positive (+) pattern of NOB-treated Ca9-22 cells. NOB increased ROS (+) (mean%) expression in Ca9-22 cells in a dose-dependent manner.

To examine the effects of NOB treatments for different amounts of time on cellular ROS levels, we treated cells with 50 μM NOB for 24, 48, or 72 hours and examined the production of ROS in each group. The data analysis results showed that the intracellular ROS levels increased with the increase in NOB treatment time, the difference was statistically significant ($n > 3$; $P < .01$). Figure 4B shows the ROS-positive (+) pattern of 50 μM NOB-treated Ca9-22 cells for different amounts of time. NOB increased ROS (+) (mean%) expression in Ca9-22 cells in a time-dependent manner.

DNA damage of NOB-treated Ca9-22 oral cancer cells

To assess the effect of treating cell with different concentrations of NOB on DNA damage, we examined the expression of the DNA damage markers γH2 AX and 8-oxodG. First, we used PCR and Western blotting to detect γH2 AX mRNA expression (Figure 5A) and protein expression (Figures 5B and 5D), with the results showing that NOB increased γH2 AX mRNA and protein expression in Ca9-22 cells in a dose-dependent manner (mean%; $n > 3$; $P < .05$). Then, we detected the 8-oxodG expression levels in Ca9-22 oral cancer cells by using an ELISA kit (Figure 5C). The results showed that NOB increased 8-oxodG expression in Ca9-22 cells in a dose-dependent manner (mean%; $n > 3$; $P < .05$).

To assess the effects of different NOB treatments for different amounts of time on DNA damage, we

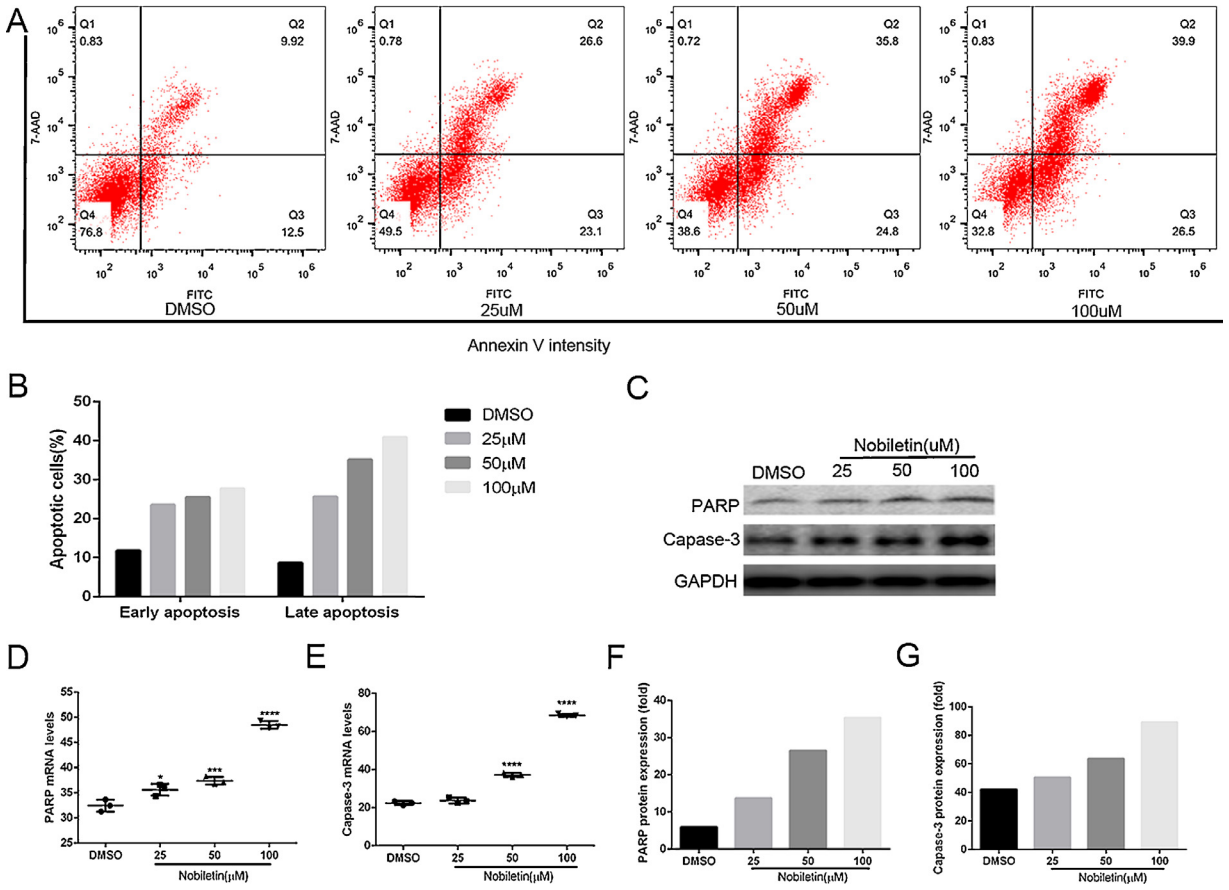

Fig. 2. Changes in the levels of apoptosis of Ca9-22 cells treated with different concentrations of nobiletin (NOB). Cells were treated with different concentrations NOB (20, 50 and 100 μM) or with dimethyl sulfoxide (DMSO) for 72 hours. **A,** Annexin V/7-AAD (7-amino-actinomycin D) flow cytometry pattern for NOB-treated Ca9-22 cells. Annexin V(+)/7-AAD(+ or −) was calculated as the apoptosis positive (+) percentage. **B,** Statistics for annexin V positive (+) (%) for (A). **C,** Poly (adenosine diphosphate-ribose) polymerase (PARP) and caspase-3 protein expression in each groups. **D,** Real-time quantitative polymerase chain reaction (RT-qPCR) for PARP messenger RNA (mRNA) expression in human oral squamous cell carcinoma (OSCC). Each bar represents the mean fold-increase in PARP mRNA compared with the DMSO groups. With the increase of NOB concentration, PARP expression gradually increased ($n > 3$; $P < .05$). **E,** RT-qPCR for capase-3 mRNA expression in human OSCC. Each bar represents the mean fold-increase in capase-3 mRNA compared with the DMSO groups. With the increase of NOB concentration, capase-3 expression gradually increased ($n > 3$; $P < .05$). **F,** The values under each lane indicate relative density of the band normalized to PARP, with use of a densitometer. **G,** The values under each lane indicate relative density of the band normalized to capase-3 with use of a densitometer.

examined the expression of DNA damage markers γH2 AX and 8-oxodG. The results showed that NOB increased γH2 AX (Figures 6A, 6B, and 6D) and 8-oxodG expression (Figure 6C) in Ca9-22 cells in a time-dependent manner (mean%; $n > 3$; $P < .05$).

DISCUSSION

In recent years, NOB has been reported to have anti-proliferative and anti-invasive activities against a variety of malignant tumor cells.[21,23] Several studies have reported the pharmacologic characteristics of NOB and its inhibitory effect on different types of tumors.[24] For example, Kandaswami et al. showed that tangeretin and NOB markedly inhibited the proliferation of a squamous cell carcinoma (HTB 43) cell line and a gliosarcoma (9 L) cell line at 2 to 8 μg/mL concentrations.[11,12] Lien et al. showed that NOB inhibits the mitogen-activated protein kinase and Akt/protein kinase B pathways and downregulates the positive regulators of the cell cycle, leading to subsequent suppression of glioma cell proliferation and migration.[25] Wu et al. showed that NOB treatment can lead to NOB and its metabolites being present in colonic tissue and that they suppressed colitis-associated colon carcinogenesis by downregulating inducible nitric oxide synthase, inducing antioxidative enzymes, and arresting cell cycle progression.[26] Sp et al. investigated the migration and invasive ability of NOB-treated endoplasmic reticulum−positive (ER[+]) cells. NOB inhibited tumor angiogenesis by regulating Src, FAK, and STAT3

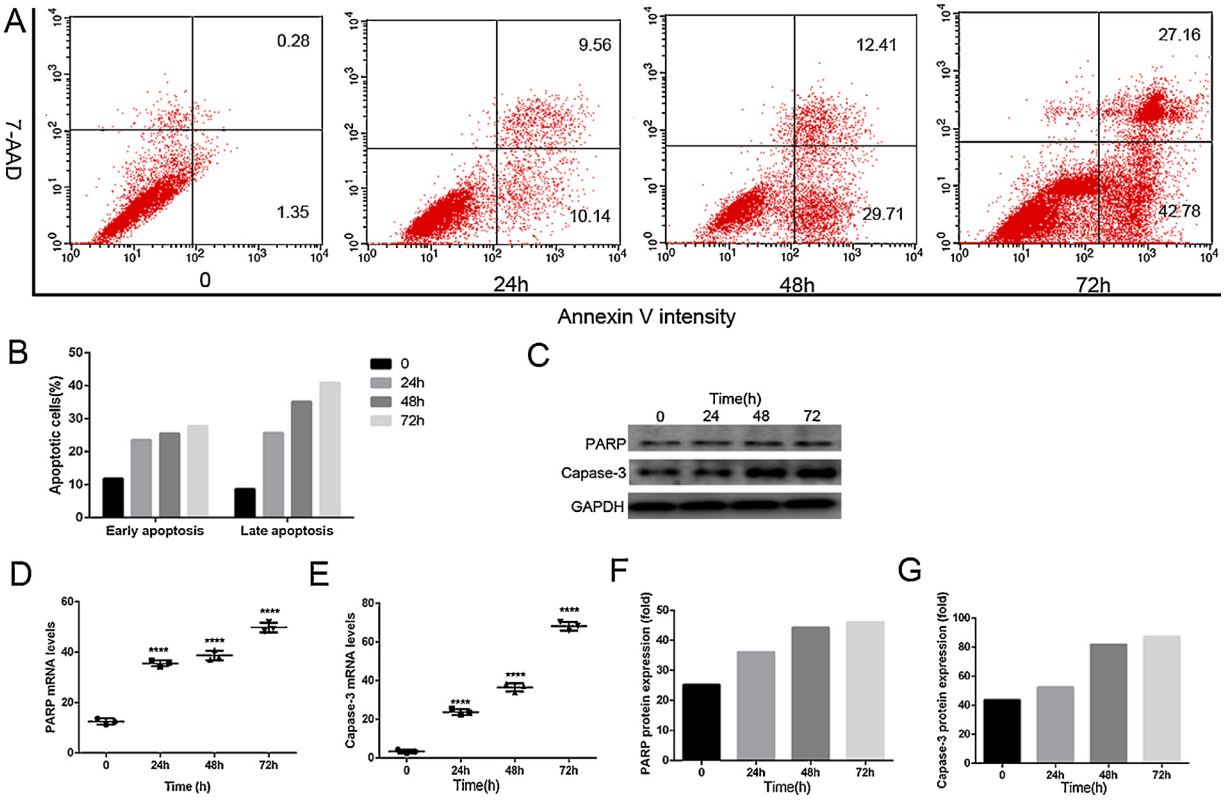

Fig. 3. Changes in the levels of apoptosis of Ca9-22 cells treated with nobiletin (NOB) for different amounts of time. Cells were treated with 50 μM NOB for 0, 24, 48, and 72 hours. **A,** Annexin V/7-AAD (7-amino-actinomycin D) flow cytometry pattern for NOB-treated Ca9-22 cells. Annexin V(+)/7-AAD(+ or −) was calculated as the apoptosis positive (+) percentage. **B,** Statistics of annexin V positive (+) (%) for (A). **C,** Poly (adenosine diphosphate-ribose) polymerase (PARP) and caspase-3 protein expression in each group. **D,** Real-time quantitative polymerase chain reaction (RT-qPCR) for PARP messenger RNA (mRNA) expression in human oral squamous cell carcinoma (OSCC). Each bar represents the mean fold-increase in PARP mRNA compared with the control groups. With the increase of treatment time, PARP expression gradually increased ($n > 3$; $P < .05$). **E,** RT-qPCR for capase-3 mRNA expression in human OSCC. Each bar represents the mean fold-increase in capase-3 mRNA compared with the control groups. With the increase of time, capase-3 expression gradually increased ($n > 3$; $P < .05$). **F,** The values under each lane indicate relative density of the band normalized to PARP with use of a densitometer. **G,** The values under each lane indicate relative density of the band normalized to capase-3 with use of a densitometer.

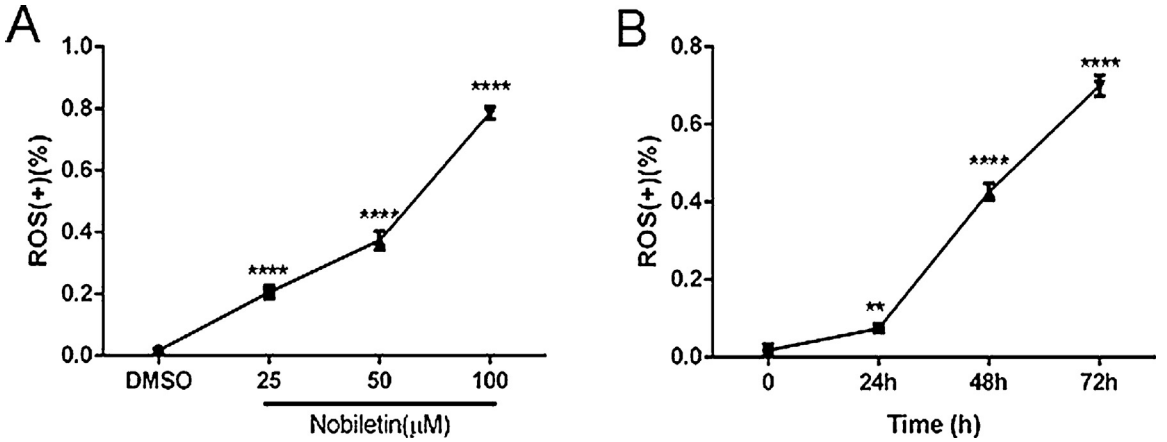

Fig. 4. Intracellular reactive oxygen species (ROS) levels of cells treated with nobiletin (NOB). **A,** The effects of different concentrations NOB on ROS production. **B,** The effects of treating cells with 50 μM NOB for different amounts of time on ROS production. Each value represents the mean of triplicate assays with standard deviation ($n > 3$; $P < .01$).

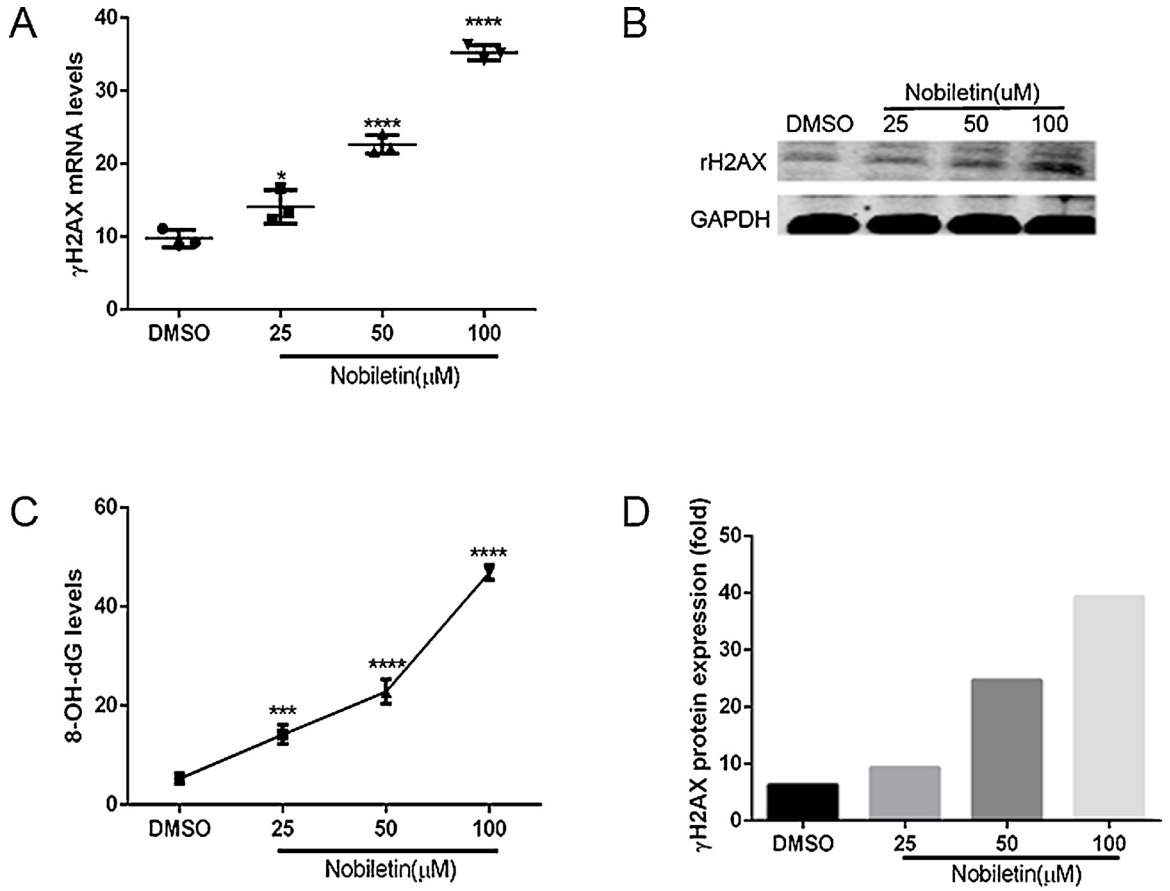

Fig. 5. Effects of different concentrations of nobiletin (NOB) on γH2 AX and 8-Oxo-20-deoxyguanosine (8-oxodG) levels in each group. **A,** Real-time quantitative polymerase chain reaction (RT-qPCR) for γH2 AX messenger RNA (mRNA) expression in human oral squamous cell carcinoma (OSCC). Each bar represents the mean fold-increase inγH2 AX mRNA compared with the dimethyl sulfoxide (DMSO) groups. With the increase of NOB concentration, γH2 AX expression gradually increased. **B,** γH2 AX protein expression. **C,** 8-oxodG expression. **D,** The values under each lane indicate relative density of the band normalized to γH2 AX with use of a densitometer ($n > 3$; $P < .05$).

signaling through PXN in ER(+) breast cancer cells.[27] However, its effect on oral cancer cells has remained unclear, and its underlying mechanism of action should be further studied. In this study, for the first time, we demonstrated that NOB prevents the proliferation of oral cancer cells by inducing apoptosis, increasing oxidative stress levels, and promoting cellular DNA damage.

In this study, we primarily assessed the effect of different concentrations of NOB (25, 50, and 100 μM) or DMSO treatments for different amounts of time (0, 24, 48, and 72 hours) on OSCC cell lines (Ca9-22, HSC-3, and TSC-15) and hOECs with respect to growth, apoptosis, ROS, and DNA damage. The results showed that as the NOB concentration and treatment time increased, the inhibition of OCSS viability significantly increased, whereas the effect on hOECs was not significant. On the basis of these results, we selected the Ca9-22 cell line for subsequent assays. We treated the cells with different concentrations of NOB for different amounts times and then assessed the levels of apoptosis, ROS, and DNA damage. The flow cytometry results showed that as the NOB concentration and time increased, the degree of cancer cell apoptosis increased. Furthermore, the levels of the apoptosis molecule PARP and caspase-3 mRNA and protein expression also increased, indicating that NOB can increase tumor cell apoptosis in a concentration- and time-dependent manner. In addition, we also showed that with the increase in NOB concentration and time, the level of ROS and the degree of DNA damage in each group also increased, indicating that NOB also stimulated the level of ROS and the degree of DNA damage in cells. In summary, NOB can inhibit the proliferation of oral cancer cells.

This study had some limitations. For instance, we did not conduct in vivo experiments to verify the inhibitory effect of NOB on oral cancer; nor did we successfully demonstrate that NOB has no effect on normal proliferative tissues at therapeutic doses. Although the

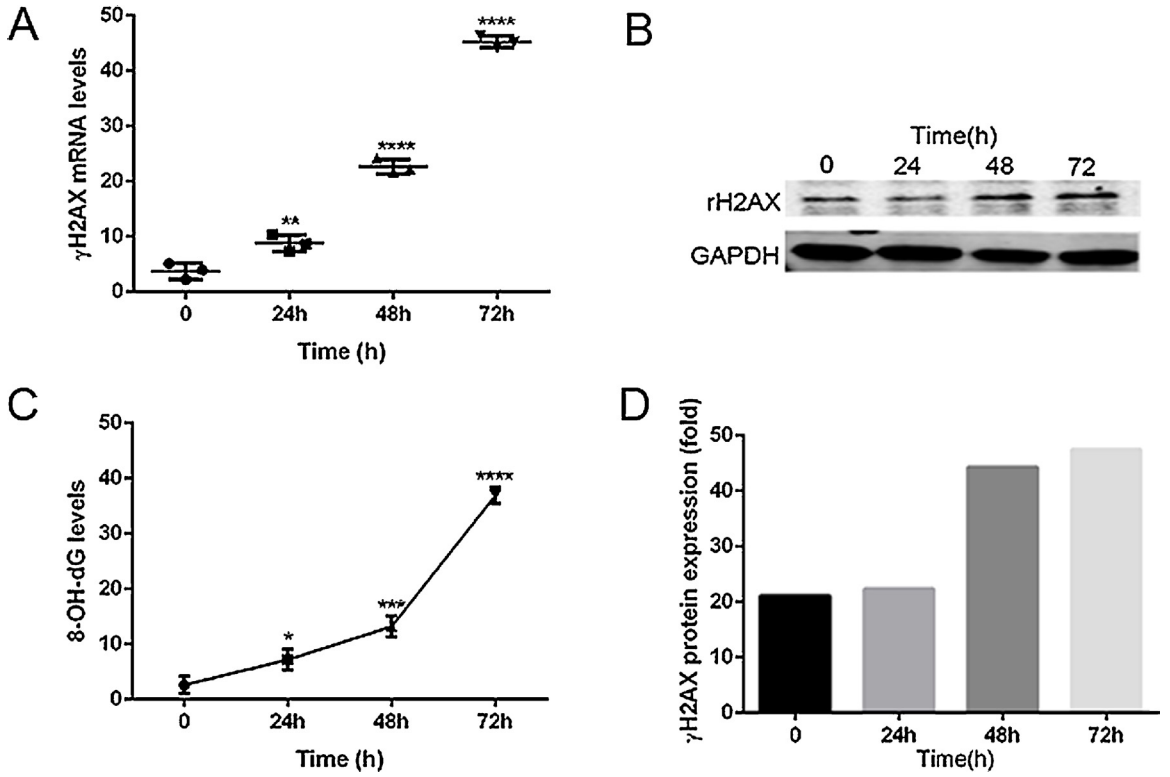

Fig. 6. Effects of treating cells with nobiletin (NOB) for different amounts of time on γH2 AX and 8-Oxo-20-deoxyguanosine (8-oxodG) expression in each group. **A,** Real-time quantitative polymerase chain reaction (RT-qPCR) for γH2 AX messenger RNA (mRNA) expression in human oral squamous cell carcinoma (OSCC). Each bar represents the mean fold-increase in γH2 AX mRNA compared with the control group. With the increase of NOB induced time, γH2 AX expression increased. **B,** γH2 AX protein expression. **C,** 8-oxodG expression. **D,** The values under each lane indicate relative density of the band normalized to γH2 AX expression with use of a densitometer ($n > 3$; $P < .05$).

results of this study showed, to some extent, that NOB may inhibit oral cancer cells, it may also affect proliferating cells other than cancer cells. These limitations will be the focus of future study.

CONCLUSIONS

The primary goal of this study was to assess the inhibitory effect of NOB on OSCC. First, using an MTT kit, NOB was observed to inhibit the activity of OSCC, after which cell apoptosis was assessed by using flow cytometry, PCR, and Western blotting assays. The results showed that with the increase in NOB concentration and time, the degree of cancer cell apoptosis increased. Subsequently, the effect of NOB on ROS levels and DNA damage was assessed, with the results showing that the level of ROS and the degree of DNA damage in each group also increased. In summary, NOB can inhibit OSCC.

ACKNOWLEDGMENTS

We sincerely thank the Department of Pathology and Stomatology, Wuhan Central Hospital (Wuhan, China), for providing us with laboratory and technical support.

REFERENCES

1. Zainal NS, Lee B, Wong ZW, et al. Effects of palbociclib on oral squamous cell carcinoma and the role of PIK3 CA in conferring resistance. *Cancer Biol Med*. 2019;16:264-275.
2. Chen MK, Liu YT, Lin JT, et al. Pinosylvin reduced migration and invasion of oral cancer carcinoma by regulating matrix metalloproteinase-2 expression and extracellular signal-regulated kinase pathway. *Biomed Pharmacother*. 2019;117:109160.
3. Velmurugan BK, Yeh KT, Hsieh MJ, et al. UNC13 C suppress tumor progression via inhibiting EMT pathway and improves survival in oral squamous cell carcinoma. *Front Oncol*. 2019;9:728.
4. Mcculloch M, Broffman M, van der Laan M, et al. Lung cancer survival with herbal medicine and vitamins in a whole-systems approach: ten-year follow-up data analyzed with marginal structural models and propensity score methods. *Integr Cancer Ther*. 2011;10:260-279.
5. Chiu CC, Haung JW, Chang FR, et al. Golden berry-derived 4 beta-hydroxywithanolide E for selectively killing oral cancer cells by generating ROS, DNA damage, and apoptotic pathways. *PLoS One*. 2013;8:E64739.
6. Saito T, Abe D, Nogata Y. Nobiletin and related polymethoxylated flavones bind to and inhibit the nuclear export factor Exportin-1 in NK leukemia cell line KHYG-1. *Biochem Biophys Res Commun*. 2020;521:457-462.
7. Wang T, Wang F, Yu L, et al. Nobiletin alleviates cerebral ischemic-reperfusion injury via MAPK signaling pathway. *Am J Transl Res*. 2019;11:5967-5977.

8. Zheng GD, Hu PJ, Chao YX, et al. Nobiletin induces growth inhibition and apoptosis in human nasopharyngeal carcinoma C666-1 cells through regulating PARP-2/SIRT1/AMPK signaling pathway. *Food Sci Nutr*. 2019;7:1104-1112.
9. Dusabimana T, Kim SR, Kim HJ, et al. Nobiletin ameliorates hepatic ischemia and reperfusion injury through the activation of SIRT-1/FOXO3 a-mediated autophagy and mitochondrial biogenesis. *Exp Mol Med*. 2019;51:51.
10. Liu F, Zhang H, Li Y, et al. Nobiletin suppresses oxidative stress and apoptosis in H9 c2 cardiomyocytes following hypoxia/reoxygenation injury. *Eur J Pharmacol*. 2019;854:48-53.
11. Kandaswami C, Perkins E, Drzewiecki G, et al. Differential inhibition of proliferation of human squamous cell carcinoma, gliosarcoma and embryonic fibroblast-like lung cells in culture by plant flavonoids. *Anticancer Drugs*. 1992;3:525-530.
12. Kandaswami C, Perkins E, Soloniuk DS, et al. Antiproliferative effects of citrus flavonoids on a human squamous cell carcinoma in vitro. *Cancer Lett*. 1991;56:147-152.
13. Liu J, Wang S, Tian S, et al. Nobiletin inhibits breast cancer via p38 mitogen-activated protein kinase, nuclear transcription factor-kappaB, and nuclear factor erythroid 2-related factor 2 pathways in MCF-7 cells. *Food Nutr Res*. 2018;62. https://doi.org/10.29219/fnr.v62.1323. eCollection 2018.
14. Wu X, Song M, Wang M, et al. Chemopreventive effects of nobiletin and its colonic metabolites on colon carcinogenesis. *Mol Nutr Food Res*. 2015;59:2383-2394.
15. Wu X, Song M, Qiu P, et al. Synergistic chemopreventive effects of nobiletin and atorvastatin on colon carcinogenesis. *Carcinogenesis*. 2017;38:455-464.
16. Tang M X, Ogawa K, Asamoto M, et al. Effects of nobiletin on PhIP-induced prostate and colon carcinogenesis in F344 rats. *Nutr Cancer*. 2011;63:227-233.
17. Sun Y, Han Y, Song M, et al. Inhibitory effects of nobiletin and its major metabolites on lung tumorigenesis. *Food Funct*. 2019;10:7444-7452.
18. Moon JY, Manh HL, Unno T, et al. Nobiletin enhances chemosensitivity to adriamycin through modulation of the Akt/GSK3 beta/beta(−)Catenin/MYCN/MRP1 signaling pathway in A549 human non-small-cell lung cancer cells. *Nutrients*. 2018;10(12).
19. Ma X, Jin S, Zhang Y, et al. Inhibitory effects of nobiletin on hepatocellular carcinoma in vitro and in vivo. *Phytother Res*. 2014;28:560-567.
20. Kawaii S, Tomono Y, Katase E, et al. Antiproliferative activity of flavonoids on several cancer cell lines. *Biosci Biotechnol Biochem*. 1999;63:896-899.
21. Ma W, Feng S, Yao X, et al. Nobiletin enhances the efficacy of chemotherapeutic agents in ABCB1 overexpression cancer cells. *Sci Rep*. 2015;5:18789.
22. Sousa DP, Pojo M, Pinto AT, et al. Nobiletin alone or in combination with cisplatin decreases the viability of anaplastic thyroid cancer cell lines. *Nutr Cancer*. 2020;72:352-363.
23. Moon JY, Cho SK. Nobiletin induces protective autophagy accompanied by ER-stress mediated apoptosis in human gastric cancer SNU-16 cells. *Molecules*. 2016;21:914.
24. Goan YG, Wu WT, Liu CI, et al. Involvement of mitochondrial dysfunction, endoplasmic reticulum stress, and the PI3 K/AKT/mTOR pathway in nobiletin-induced apoptosis of human bladder cancer cells. *Molecules*. 2019;24:2881.
25. Lien LM, Wang MJ, Chen RJ, et al. Nobiletin, a polymethoxylated flavone, inhibits glioma cell growth and migration via arresting cell cycle and suppressing MAPK and Akt pathways. *Phytother Res*. 2016;30:214-221.
26. Wu X, Song M, Gao Z, et al. Nobiletin and its colonic metabolites suppress colitis-associated colon carcinogenesis by down-regulating iNOS, inducing antioxidative enzymes and arresting cell cycle progression. *J Nutr Biochem*. 2017;42:17-25.
27. Sp N, Kang DY, Joung YH, et al. Nobiletin inhibits angiogenesis by regulating Src/FAK/STAT3-mediated signaling through PXN in ER(+) breast cancer cells. *Int J Mol Sci*. 2017;18:935.

Reprint requests:

Minghui Pan
Department of Stomatology
The Central Hospital of Wuhan
No. 26 Shengli Street
Jiang'an District
Wuhan
China
Minghuipan123@163.com